ELSEVIER

Journal of Chromatography A, 795 (1998) 185–198

JOURNAL OF CHROMATOGRAPHY A

Non-linear elution effects in split-peak chromatography II. Role of ligand heterogeneity in solute binding to columns with adsorption-limited kinetics

John G. Rollag, David S. Hage*

Department of Chemistry, University of Nebraska, Lincoln, NE 68588-0304, USA

Received 24 June 1997; received in revised form 16 September 1997; accepted 16 September 1997

Abstract

The split-peak effect is a useful phenomenon in studying the kinetic behavior of chromatographic supports. This work examined the combined role of ligand heterogeneity and non-linear elution conditions (i.e., sample load dependence) on the solute free fractions that are measured during split-peak studies. Exact expressions were derived to describe the effects of ligand heterogeneity under linear elution conditions, and simulation models were developed to specifically examine the combined effects of ligand heterogeneity and non-linear elution in systems with adsorption-limited rates for solute binding. The simulations showed that ligand heterogeneity increased the amount of free solute seen at any flow-rate or sample size, with this being most noticeable when using low flow-rates or large samples. One application in which these increases were examined in detail concerned the use of the split-peak effect for association rate constant measurements. It was found that linear extrapolation methods developed for homogeneous systems (as a correction for non-linear elution conditions) could successfully be applied to columns containing heterogeneous ligands. Columns containing immobilized protein A and/or protein G were used as experimental models to test the validity of the simulations; the behavior of these columns showed good quantitative and qualitative agreement with the predicted theoretical results. © 1998 Elsevier Science B.V.

Keywords: Ligand-heterogeneity; Split-peak effect; Stationary phases, LC; Adsorption; Kinetics; Proteins

1. Introduction

The role of non-linear elution conditions in chromatography remains an area of continuing interest in both preparative and analytical-scale work. In general, non-linear elution can be said to occur whenever there is a change in the chromatographic response or behavior of a solute as the amount of applied solute is increased [1]. The split-peak effect is one phenomenon in which non-linear conditions can be important [2–6]. This phenomenon was first predicted by Giddings and Eyring in 1955 [7] and has since been observed in a number of chromatographic systems [2–4,6,8–14]. It is characterized by the production of two fractions from the injection of a single solute, with the first fraction representing solute that passes through the column non-retained and the second fraction representing solute that is bound by the column. Such behavior is produced by slow kinetics and/or insufficient time for the solute to bind as it travels through the chromatographic system. The extent of this effect is determined by such things as the mass transfer and association rate constants for

*Corresponding author.

0021-9673/98/$19.00
PII S0021-9673(97)00975-8

the solute, the amount of binding sites in the column and the column size or sample application flow-rate [2–5]. Although the split-peak effect can potentially occur in any type of column, it tends to be most pronounced in work with affinity supports because of their relatively low ligand densities and slow solute–ligand association kinetics [2].

The split-peak effect has previously been employed in the measurement of solute–ligand association or adsorption rate constants and solute diffusion coefficients [2,6,8,10,11,14]. It has also been used in the design and optimization of various high-performance affinity chromatographic assays [9,12,13,15–17]. The understanding of this effect has been greatly aided by the availability of equations and theory that relate the amount of free (or non-retained) solute to such factors as the mass transfer and adsorption rates for the solute, as well as the relative sample load and application flow-rate [2–5,9,10]. However, these equations have focused exclusively on the case in which a homogenous population of binding sites is present in the column. Although such expressions show good qualitative agreement with trends observed in experimental systems, their predicted free fractions tend to be much lower than those seen in practice. Ligand heterogeneity has often been proposed as a reason for these observed differences [2–4,8,9,14], but no previous theoretical work has examined the actual role that such heterogeneity plays in split-peak measurements.

This present work will study how the amount of non-retained solute changes in the split-peak effect when various degrees of ligand heterogeneity are introduced into a column. The specific case that will be considered is one in which adsorption-limited kinetics are present (i.e., solute adsorption to the stationary phase is the rate-limiting step in retention). Such a situation is of particular interest in affinity chromatography, where both slow adsorption rates and heterogeneous ligands can often be present [2]. Initial experiments in this study will use computer simulations and work with chromatographic theory to predict the changes expected in split-peak behavior in going from a one to two ligand system. The results will then be compared to experimental data obtained for high-performance affinity columns based on protein A, protein G or mixed-bed protein A and G supports.

2. Theory

2.1. Split-peak effect for columns with homogeneous ligands

The reactions shown in Eqs. (1) and (2) can be used to describe the mass transfer and adsorption of a solute (A) to an immobilized ligand (L) as the solute passes through a chromatographic column [2,3,18]:

$$\mathrm{A} \underset{k_{-1}}{\overset{k_1}{\rightleftarrows}} \mathrm{A} \tag{1}$$

$$\mathrm{A} + \mathrm{L} \xrightarrow{k_3} \mathrm{A} - \mathrm{L} \tag{2}$$

In this model, k_1 and k_{-1} are the forward and reverse rate constants that describe the mass transfer of solute from the flow mobile phase (i.e., the solvent outside the pores of the support) to the stagnant mobile phase (i.e., the mobile phase within the pores or directly in contact with the support's surface). The term k_3 represents the second-order association or adsorption rate constant for the binding of solute with the immobilized ligand. A dissociation rate constant can also be included as part of Eq. (2) for systems with reversible binding; however, this process is often assumed to be negligible for systems with slow-dissociation (e.g., many types of affinity columns), especially on the short time scales characteristic of most split-peak studies [2,3].

An equation has previously been developed for work under linear elution conditions (i.e., when using infinitely small amounts of sample) that describes the relative fraction of non-retained solute (f) that would be expected for a chromatographic system with either mass transfer- or adsorption-limited kinetics; the result is shown below in Eq. (3) [2]:

$$-1/\ln f = F[1/(k_1 V_e) + 1/(k_3 m_L)] \tag{3}$$

In this expression, F is the flow-rate used for sample injection, V_e is the excluded volume of the column (i.e., the flowing mobile phase volume), and m_L is the moles of active immobilized ligand in the column. In the case where the rate of solute adsorption is much slower than solute diffusion or mass transfer (i.e., $1/k_1V_e \ll 1/k_3m_L$), Eq. (3) reduces to

$$-1/\ln f = F/(k_3m_L) = S_o \quad (4)$$

or

$$f = e^{-1/S_o} \quad (5)$$

where S_o is a combination of system parameters referred to as the split-peak constant [12]. Note that Eq. (4) predicts a linear relationship between $-1/\ln f$ and F with a slope of $(1/k_3m_L)$ and an intercept of zero. Through this relationship, it has been shown that association rate constants can be measured by the split-peak effect [2,3]. Similarly, a plot of $-1/\ln f$ versus S_o for an infinitely dilute sample should result in a dimensionless plot with a slope of one and an intercept of zero; by expanding this type of plot to finite samples (i.e., non-linear conditions), the result is a series of universal curves that indicate the effects of non-linear elution on split-peak measurements performed with columns containing homogeneous ligands [3]. The same general type of plot will be used in this study to examine the combined effects of non-linear elution and ligand heterogeneity in split-peak determinations.

When working with a system that has adsorption-limited kinetics for solute retention, Eq. (5) can be expanded to include the case in which a finite or non-infinitely dilute sample is being applied to the column [5,12].

$$f = (S_o/\text{Load A})\ln[1 + (e^{\text{Load A}/S_o} - 1)e^{-1/S_o}] \quad (6)$$

In this new expression, Load A is the relative moles of solute applied to the column versus the total moles of active ligand and all other terms are the same as defined earlier. Although the relationship in Eq. (6) can be applied to a broader range of conditions than Eq. (5), it still assumes that a homogenous population of ligands is present in the column.

2.2. Split-peak effect for columns with heterogeneous ligands

The reaction shown in Eq. (2) for the homogeneous case can be modified as follows to describe the retention of solute A onto a column that contains a mixture of ligands (L_1 through L_n) distributed uniformly throughout the column:

$$A + L_1 \overset{k_{31}}{\rightarrow} A - L_1 \quad (7)$$

$$\vdots$$

$$A + L_n \overset{k_{3n}}{\rightarrow} A - L_n \quad (8)$$

In Eqs. (7) and (8), k_{31} through k_{3n} are the association rate constants for ligands L_1 through L_n arranged in order of decreasing size, with $k_{31} > k_{32} \ldots > k_{3n}$. The mass transfer of solute from the flowing mobile phase to the stagnant mobile phase is the same in this model as in Eq. (1), but the solute that enters the stagnant mobile phase can now react with any one of several different ligands that make up the stationary phase. One assumption still made in the above scheme is that the immobilized ligands are independent of one another and that the values of k_{31} through k_{3n} are not affected by solute binding to other ligands (i.e., no allosteric or steric hindrance effects are present).

It is possible to use the same general approach as employed in obtaining Eqs. (3)–(5) to determine the free fraction expected under linear elution conditions for a column containing a heterogeneous ligand population. The results, as derived in Appendix A, are summarized in Eqs. (9)–(11).

General heterogeneous case, linear elution conditions

$$-1/\ln f = F\left[1/(k_1V_e) + 1/\left(\sum\{k_{3i}m_{Li}\}\right)\right] \quad (9)$$

$$= F\left[1/(k_1V_e) + 1/\left(k_{31}m_{Ltot}\sum\{\alpha_i\beta_i\}\right)\right] \quad (10)$$

Adsorption-limited heterogeneous case, linear elution conditions

$$-1/\ln f = F/\left(k_{31} m_{\mathrm{Ltot}} \sum \{\alpha_i \beta_i\}\right) = S_{\mathrm{o}} \qquad (11)$$

In the above equations all summations are given over the range $i=1$ to n for a column containing n-types of ligands. The terms $m_{\mathrm{L}i}$ and k_{3i} represent the moles of ligand site i and its corresponding association rate constant for the injected solute. The term m_{Ltot} is the total moles of all active ligands present in the column ($\Sigma m_{\mathrm{L}i}$), α_i is the fraction of all binding sites that are represented by ligand i ($m_{\mathrm{L}i}/m_{\mathrm{Ltot}}$), and β_i describes the relative size of rate constant k_{3i} versus the largest association rate constant for the solute with any ligand in the column (k_{31}), where $\beta_i = k_{3i}/k_{31}$. Note that, like the expressions given in Eqs. (3) and (4) for the homogeneous case, Eqs. (9)–(11) predict a linear relationship for $-1/\ln f$ versus F (or S_{o}) with an intercept of zero when using an infinitely dilute sample (i.e., linear elution conditions). However, the difference between Eqs. (3) and (4) and Eqs. (9)–(11) is that plots for the heterogeneous case will now have slopes that are a function of both the association rate constants for all ligands and the relative amount of each ligand in the column.

Although an exact solution is not yet available for describing the split-peak effect when working with heterogeneous ligands and finite sample loads (or non-linear conditions), such a system can be modeled by computer simulations. This can be done through an approach similar to that described for columns with a homogeneous stationary phase [3]. Such simulations are based on a modified Craig distribution in which the column length is divided into a series of slices, which in turn are further divided into three distinct regions corresponding to the flowing mobile phase, stagnant mobile phase and stationary phase. The simulation is begun by applying sample to the flowing mobile phase region of the first slice in the column; this is followed by distribution of the solute for a given interval of time between the various phases in each slice based on a predetermined set of kinetic equations. In this work, the simulation was performed by placing the flowing and stagnant mobile phase regions in equilibrium (i.e., fast mass transfer kinetics) and by having solute within the stagnant mobile phase adsorb to ligands in the stationary phase according to the following differential equations:

$$-d[\mathrm{L}_1]/dt = k_{31}[\mathrm{A}][\mathrm{L}_1] \qquad (12)$$

$$\vdots$$

$$-d[\mathrm{L}_n]/dt = k_{3n}[\mathrm{A}][\mathrm{L}_n] \qquad (13)$$

In the above equations, $[\mathrm{L}_1]$ through $[\mathrm{L}_n]$ represent the effective concentration of each immobilized ligand at time t within the stagnant mobile phase or pore volume (V_{p}) of a given slice, where $[\mathrm{L}_i] = m_{\mathrm{L}i}/V_{\mathrm{p}}$. In the same fashion, [A] represents the molar concentration of solute within the stagnant mobile phase region of the slice at time t. Although there is no exact expression that can be used as a general solution to Eqs. (12) and (13), this system can still be solved by using numerical integration techniques. This was accomplished here by using a fourth-order Runge–Kutta method (see Ref. [19] for details on this technique) to solve the above differential equations and to determine the degree of solute adsorption within each slice along the length of the column.

After the solute is allowed to distribute in all slices for a given period of time, the simulation is continued by moving the solute in the flowing mobile phase region of each slice into the same region of the next slice in order to simulate solvent flow through the column. As this is done, the amount of solute that elutes from the last slice is monitored, giving rise to a chromatogram for the system. In determining the amount of solute that eluted non-retained from the column (i.e., the free fraction f), the simulations in this work were conducted until all but one-trillionth of the originally-applied solute had either irreversibly adsorbed to the stationary phase or had eluted from the column. During the simulation the total amount of solute on or off the column was also continuously monitored by summing the solute present in all slices and phase regions; this was done to detect and avoid the occurrence of any round-off or truncation errors as a result of the simulation.

3. Materials and methods

3.1. Reagents

The protein A (recombinant single binding domain), protein G (recombinant intact protein) and rabbit immunoglobulin G (IgG) were obtained from Sigma (St. Louis, MO, USA). The Nucleosil Si-1000 silica (7 μm particle size, 1000 Å pore size) was from P.J. Cobert (St. Louis, MO, USA). Other chemicals were of the highest grades available. All solutions and samples were made using deionized water generated by a Nanopure water system (Barnstead, Dubuque, IA, USA).

3.2. Instrumentation

All simulations were performed using programs written in Microsoft QuickBasic or Fortran (Microsoft, Seattle, WA, USA) and were run on a 386 IBM-based 25 MHz computer or a 3600 Vax mainframe computer, respectively. The high-performance liquid chromatography (HPLC) system employed in the protein A and G studies consisted of two model CM3000 HPLC pumps from Thermoseparations (Riviera Beach, FL, USA) for use with the sample application and elution buffers. Sample injection was performed using a Rheodyne 7010 valve (Cotati, CA, USA) equipped with a 28 μl calibrated injection loop and a VICI DVI actuator switching module from Chromtech (Apple Valley, MN, USA). Elution of rabbit IgG was monitored at 280 nm using a model SM3100 UV–Vis variable wavelength detector from Thermoseparations, and the resulting data were collected using Winner-on-windows software, also from Thermoseparations.

3.3. Computer simulations

The computer algorithm employed in this work was similar to that described for previous simulations of the split-peak effect [3] but was now modified for use with the Runge–Kutta numerical integration method [19]. The accuracy and convergence of the simulations were tested by using the homogenous case described in Eq. (6) and Ref. [3] as a reference. As the number of slices within the simulated columns was increased, the free fraction values obtained in simulations of the homogeneous case were found to quickly approach the true values predicted by Eq. (6); however, the simulation time also increased as more slices were used per column. As a compromise between these two factors, a column length of 320 slices was used in all further simulation work. It was estimated that such conditions gave an error of less than 0.5 ppt in the final free fractions obtained by the simulations performed in this study.

3.4. Chromatography

The protein A and protein G supports were prepared according to previous methods by using the Schiff base immobilization technique and diol-bonded Nucleosil Si-1000 as the starting material [2,3,9]. The final protein A, protein G or mixed-bed protein A–protein G supports were downward slurry-packed at 3500 p.s.i. into separate 6.35 mm×2.1 mm I.D. stainless steel columns. Samples of rabbit IgG were applied to these columns in pH 7.0, 0.10 *M* phosphate buffer and were later eluted by using a pH 2.5, 0.10 *M* phosphate buffer. The split-peak studies were performed by measuring the non-retained or free fractions of rabbit IgG obtained on each column over flow-rates ranging from 0.1 to 2.5 ml/min. The area of each non-retained peak was measured and the corresponding free fraction was calculated by comparing this area to that measured at the same flow-rate when injecting an identical sample onto a 6.35 mm×0.25 mm I.D. column containing only diol-bonded Nucleosil Si-1000 (i.e., a support with no retention for rabbit IgG).

The binding capacity of each column (m_{Ltot}) was determined by frontal analysis. This was performed at flow-rates of 0.1–0.2 ml/min by continuously applying $1.1–7.5\cdot10^{-7}$ *M* rabbit IgG in pH 7.0, 0.10 *M* phosphate buffer to each test column. Similar studies were performed on the diol-bonded Nucleosil column in order to correct for the void time of the HPLC system. The resulting breakthrough data were then processed as described in Refs. [2,9] to determine the value of m_{Ltot} for each column.

4. Results and discussion

One common format used in split-peak studies

involves determining the non-retained fraction that is produced as a constant amount of solute is injected at several different flow-rates onto a column. An example of such a study is shown in Fig. 1 for the injection of rabbit IgG onto a protein G support. In this type of experiment the relative amount of non-retained solute that passes free through the column will increase as the flow-rate of application is increased, or as the column residence time is decreased. These non-retained peak areas are then compared to the total areas measured for an identical sample injected at the same flow-rates onto a column that has no retention for the solute (e.g., see diol-bonded silica column results in Fig. 1). From these data, the relative free fraction of the solute can be calculated and plotted as a function of flow-rate, as shown in Fig. 2. Note that the general response seen for the graphs in Fig. 2 is the same as predicted by Eqs. (3) and (4) and Eqs. (9)–(11), in which a linear relationship in obtained between $-1/\ln f$ and F with an intercept at or near zero. This linear behavior agrees with results reported in earlier work with protein A columns [2,3] and was found to occur for all of the columns, sample loads, and flow-rate conditions used throughout this study.

The role of ligand heterogeneity in altering the shape and response of graphs like those in Fig. 2 was

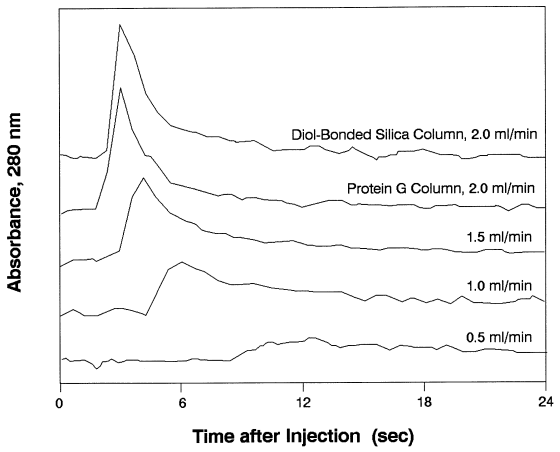

Fig. 1. Non-retained or free fractions observed in split-peak measurements for the injection of rabbit IgG (volume, 28 μl; Load A, 0.1 mol IgG/mol protein G) onto a 6.35 mm×2.1 mm I.D. diol-bonded silica column at 2.0 ml/min, or a 6.35 mm×2.1 mm I.D. protein G silica column at flow-rates of 0.5–2.0 ml/min.

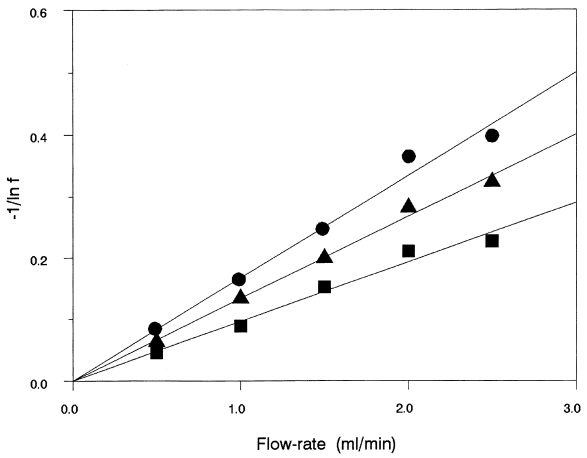

Fig. 2. Typical split-peak plots of $-1/\ln f$ versus flow-rate for the injection of rabbit IgG (volume, 28 μl; Load A, 0.1 mol IgG/mol ligand) onto 6.35 mm×2.1 mm I.D. columns containing immobilized protein A (■), protein G (●) or a mixed-bed protein A–protein G support (▲).

first examined by considering the case in which two distinct types of ligands are present in the column. For this situation, Eq. (11) can be rewritten as

$$-1/\ln f = F/(k_{31} m_{\mathrm{Ltot}}\{\alpha_1 + \beta_2 - \alpha_1\beta_2\}) = S_{\mathrm{o}} \quad (14)$$

where the number of variables indicating the extent of column heterogeneity has now been reduced to only two (α_1 and β_2) by using the fact that $\alpha_2 = (1-\alpha_1)$ and $\beta_1 = k_{31}/k_{31} = 1$. These two remaining factors represent the degree of heterogeneity in either the relative amount of each ligand in the column (α_1) or in the association rate constants for these ligands (β_2).

Before considering the effects of ligand heterogeneity, it is helpful to reexamine the changes that occur in the solute free fraction on a homogeneous column as a function of flow-rate or S_{o} (since $S_{\mathrm{o}} = F/\{k_3 m_{\mathrm{L}}\}$) and the amount of injected sample (Load A). Such a case is illustrated in Fig. 3(a and c). These plots represent two different types of split-peak studies, referred to here as the constant sample load (Fig. 3a) and constant flow-rate methods (Fig. 3c). Both formats have been used in previous work with the split-peak effect to study solute adsorption to various chromatographic supports [2,3,6,9–11,14–17]. As noted earlier [2,3], the presence of non-linear

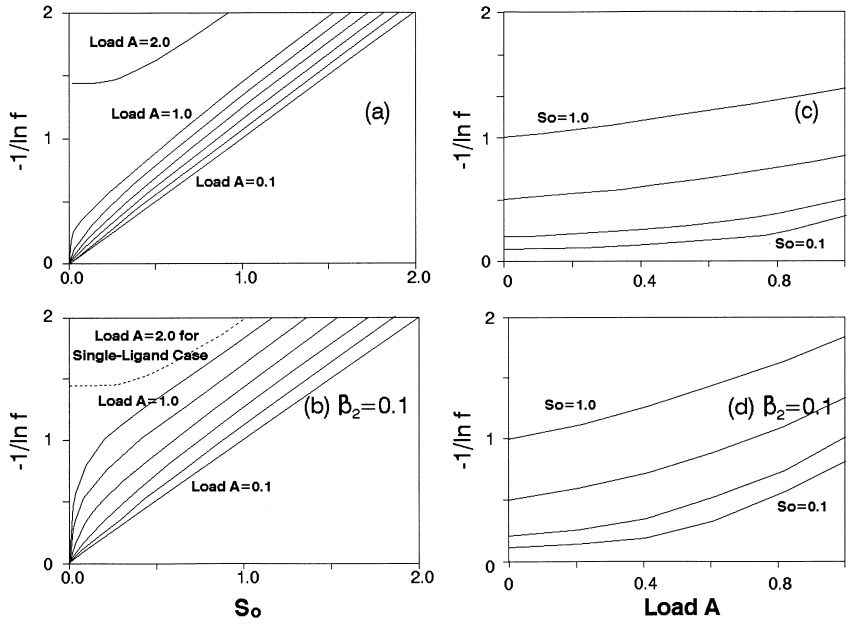

Fig. 3. Predicted effect of ligand heterogeneity on split-peak plots prepared for constant sample load (a,b) or constant flow-rate (c,d) experiments. The plots in (a) and (c) were generated by Eq. (6) and represent the homogeneous case in which only one type of ligand is present in the column ($\alpha_1 = 1$ and/or $\beta_2 = 1$). The plots in (b) and (d) were generated by the computer model and are for a heterogeneous case in which an equal amount of two different ligands is present ($\alpha_1 = \alpha_2 = 0.5$) but with the association rate constant for the second ligand being only one-tenth that of the first ($\beta_2 = 0.1$). The solid lines in (a) and (b), from bottom to top, were obtained at relative solute loads of 0.01, 0.2, 0.4, 0.6, 0.8 and 1.0; the top solid line in (a) and dashed line in (b) were obtained at a load of 2.0 for the homogeneous case represented in (a). The solid lines in (c) and (d), from bottom to top, were obtained at S_o values of 0.1, 0.2, 0.5 and 1.0.

elution in the homogeneous case results in an increase in the value of $-1/\ln f$ (and the free fraction f) at all flow-rates or S_o values. The greatest change in $-1/\ln f$ occurs at high sample loads, but even small amounts of sample produce deviations from the behavior expected under true linear elution conditions (i.e., an infinitely dilute sample) [3].

The way in which this behavior changes in the presence of heterogeneous ligands is indicated by Fig. 3(b and d). These particular graphs were generated for the case in which there are identical amounts of two different ligands in the column ($\alpha_1 = \alpha_2 = 0.5$), with the second type of ligand having a solute association rate constant that is only one-tenth that of the first ($\beta_2 = 0.1$). In the constant sample load experiment for this case (Fig. 3b), the values of the free fraction and $-1/\ln f$ shift to higher levels for each combination of flow-rate and sample load. The same type of behavior is seen for ligand populations having other α_1 and β_2 values, with the extent of this increase becoming largest at low flow-rates (i.e., small S_o values) or high sample loads. Similar trends are found in the constant flow-rate experiments (Fig. 3d). Thus, these results indicate that ligand heterogeneity is indeed a possible explanation for the larger-than-expected free fractions observed in previous split-peak studies [2–4,8,14].

A comparison of Fig. 3(a and b) gives some insight regarding the relative importance of fast versus slow binding ligands in split-peak studies. For example, at high or intermediate flow-rates and S_o values, the plot in Fig. 3b at Load A = 1.0 for an equal amount of two different ligands approaches the response seen in Fig. 3a at twice the sample load for a single class of ligand sites. Such behavior is most notable when working with a mixture of ligands that have a large difference in their association rate constants (i.e., $\beta_2 < 0.2$). This suggests that the injected solute is not effectively sampling the slower

binding ligands under these conditions, thus leading to a column that mimics a homogeneous support. This hypothesis is supported by the fact that Eq. (6), which is based on a homogeneous model, gives a relatively good fit to all of the curves shown in Fig. 3b at S_o values above 0.5–1.0. Conversely, at low flow-rates and S_o values, Eq. (6) does not provide a good description of the plots in Fig. 3b. This indicates that the time spent by the sample within the column at these lower flow-rates is now sufficiently long for the solute to show significant adsorption to the slower binding ligand; the result is a greater effect due to ligand heterogeneity under such experimental conditions.

The graphs in Fig. 3 were constructed using S_o as the independent variable; as indicated earlier in Eqs. (11) and (14), this approach normalizes for any changes in the absolute values of the association rate constants or column binding capacities for a multiligand system and allows universal plots to be generated that illustrate the overall role played by ligand heterogeneity in split-peak measurements. However, the use of S_o as the *x*-parameter does require prior knowledge of the degree of ligand heterogeneity that exists in the system. This creates a slight problem in applying these results directly to real chromatographic columns because for many column supports the extent of ligand heterogeneity, or even the existence of such heterogeneity, is not usually known in advance.

When using the constant sample load method in split-peak studies, it has been suggested previously that one possible way of detecting ligand heterogeneity in a real system may be to plot $-1/\ln f$ versus flow-rate and examine how the observed slopes change with the amount of applied sample [3]. For a constant flow-rate study, an analogous experiment would be to plot $-1/\ln f$ versus sample load at each of several application flow-rates. The results can then be compared to those predicted by Eq. (6) for a true homogeneous system. Fig. 4 shows examples of such plots generated for several different values of β_2 on a column with identical amounts of two types of ligands. Note that the dimensionless term $F/(k_{31}m_{Ltot})$ is used in these graphs instead of F for the sake of convenience; similar qualitative behavior is seen regardless of whether F or $F/(k_{31}m_{Ltot})$ is employed. The graphs in Fig. 4 indicate

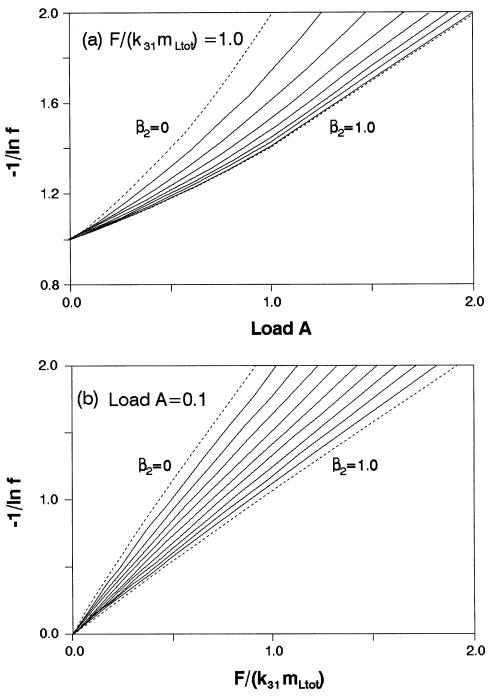

Fig. 4. Predicted effect of ligand heterogeneity on split-peak plots prepared as a function of flow-rate, or a normalized flow-rate $F/(k_{31}m_{Ltot})$. The plots shown in (a) and (b) are for the constant flow-rate and constant sample load experiments, respectively. All of the solid lines are data obtained by computer simulations for a case in which an equal number of two ligands are present in the column ($\alpha_1=\alpha_2=0.5$). The solid lines in (a), from left to right, represent values for β_2 (the association rate constant heterogeneity) of 0.1, 0.2, 0.3, 0.4, 0.5, 0.6 and 0.8; the solid lines in (b), from left to right, represent β_2 values of 0.1, 0.2, 0.3, 0.4, 0.5, 0.6, 0.7, 0.8 and 0.9. The dashed lines in (a) and (b) show the results expected according to Eq. (6) for a homogeneous column as β_2 approaches zero (i.e., the second type of ligand is inactive) or β_2 approaches one (i.e., the two ligands have identical association rate constants and therefore act kinetically as a single type of site).

that as more heterogeneity is introduced into the ligand association rate constants (i.e., as β_2 decreases), the slopes for plots of $-1/\ln f$ versus flow-rate (Fig. 4b) will increase. This result gives good agreement with previous observations made in split-peak studies performed on affinity columns that had comparable binding capacities but known differences in ligand heterogeneity [2,3]. Likewise, in a constant flow-rate study (Fig. 4a) the measured value of $-1/\ln f$ at any given sample load would be expected to increase as the value of β_2 decreases. The same general types of changes are seen when

varying the relative amount of each ligand (i.e., as β_2 is held constant and α_1 is changed – data not shown). A more detailed assessment of how the slopes for such plots change with various degrees of ligand heterogeneity is currently under investigation (manuscript in preparation).

One interesting observation that can be made from Fig. 4 and related graphs is that the value of $-1/\ln f$ will increase only to a certain maximum level in work with any heterogeneous system. For example, as β_2 is decreased the upper limit for $-1/\ln f$ at a given flow-rate or value of Load A will occur at the point where the association rate constant for the second ligand becomes so slow that the binding of solute to this ligand is essentially negligible on the time-scale of the split-peak experiment. Under these conditions the column behaves like a homogeneous system and follows the behavior predicted by Eq. (6) (e.g., see dashed lines given in Fig. 4 for $\beta_2 = 0$). The same shift from heterogeneous to homogeneous behavior is seen when changing the relative amount of each ligand and occurs as the value of α_1 approaches either one (i.e., only the fastest binding site is present in the column) or zero (i.e., only the slower binding ligand is present).

A specific application reported for the split-peak effect has been its use in the measurement of association rate constants for immobilized ligands in affinity columns [2,3,8,14,15]. One approach for doing this is to prepare graphs of $-1/\ln f$ versus flow-rate under conditions in which the rate of solute mass transfer is faster than that of solute–ligand adsorption (i.e., $1/\{k_1 V_e\} < 1/\{k_3 m_L\}$ in Eq. (3)). In order to correct for non-linear elution conditions, the graphs of $-1/\ln f$ versus flow-rate are prepared at several sample loads and the resulting slopes are plotted versus the amount of injected sample (e.g., see Figs. 5 and 6). The intercept of this second plot gives the ''extrapolated split-peak slope'', or the true value for $1/\{k_3 m_L\}$ (Note: if $1/\{k_1 V_e\}$ is not negligible, then independent estimates of this term must be used along with the intercept to provide $1/\{k_3 m_L\}$) [2]. By combining the resulting value for $1/\{k_3 m_L\}$ with independent estimates of m_L, the association rate constant k_3 is then obtained [2,3].

Previous theoretical studies have confirmed the accuracy of this extrapolation technique for the correction of non-linear elution in split-peak association rate constant measurements of homogeneous columns [3]; however, no work has yet been performed examining the accuracy of the same approach when applied to columns with heterogeneous ligands. The effect of ligand heterogeneity on the accuracy of this method was tested here by using computer simulations to generate plots of $-1/\ln f$ versus S_o for various sample loads and combinations of α_1 and β_2. Typical simulation results for homogeneous and heterogeneous columns are shown in Fig. 5. Some curvature at high sample loads (Load A $\geq$ 0.3) can be seen in Fig. 5 for both the homogeneous and heterogeneous systems, with the heterogeneous case showing a larger sample load dependence, as predicted from Fig. 4. But at lower sample loads (Load A $\leq$ 0.2) a linear relationship is present between the measured slopes and amount of applied sample; it is these conditions that are most easily

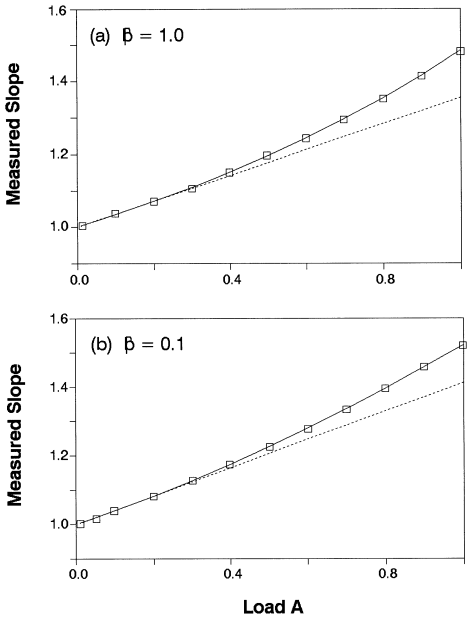

Fig. 5. Change in the slopes measured for simulated plots of $-1/\ln f$ versus S_o at various amounts of applied sample (Load A) for (a) a column with homogeneous ligands, using data generated by Eq. (6), or (b) a column containing equal amounts of two different ligands ($\alpha_1 = \alpha_2 = 0.5$) that have a ten-fold difference in association rate constants, using data generated by the computer model. The dashed line in each plot shows the best-fit linear response over a Load A range of 0.01–0.2. Each square in these plots represents a slope measured over 17 data points between S_o values of 0.01 and 1.25.

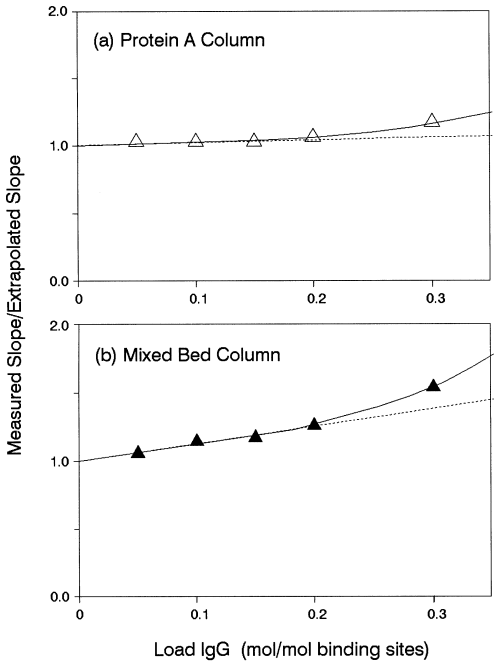

Fig. 6. Actual change in the experimental slopes measured for plots of $-1/\ln f$ versus flow-rate at various amounts of applied sample (Load IgG) for (a) a recombinant protein A column or (b) a mixed-bed recombinant protein A–protein G column. For ease of comparison with Fig. 5, all *y*-axis values in these graphs were normalized to an intercept value of 1.0 by dividing them by the extrapolated split-peak slope (i.e., the intercept obtained from the best-fit line shown at the four smallest Load A values). The dashed line in each plot shows the best-fit linear response over Load A values of 0.05–0.2. Each triangle represents a slope measured over five data points between flow-rates of 0.5 and 2.5 ml/min.

used to obtain the extrapolated split-peak slope at zero sample load [3]. This linear region was observed for all of the homogeneous and heterogeneous cases that were tested, with typical correlation coefficients of 0.999 or greater ($n=4$–5) over Load A values of 0.01–0.20. This behavior is in good agreement with previous observations made when using these types of plots to examine the split-peak behavior of protein A affinity columns [2,3].

The actual intercept expected for the plots in Fig. 5 was 1.0, which (according to Eqs. (4) and (11)) is the slope expected for graphs of $-1/\ln f$ versus S_o under true linear elution conditions. It can be seen from Fig. 5(a and b) that the best-fit lines over the Load A region of 0.01–0.20 gave close agreement to this expected result for both the heterogeneous and homogeneous systems. By comparing the actual and expected intercepts for such graphs, it was possible to determine the accuracy of this extrapolation method. For the heterogeneous system, all combinations of α_1 and β_2 gave an error of less than $\pm 0.1\%$, and most gave an error of less than $\pm 0.03\%$. Similar accuracy has been reported earlier when using the same approach for the homogeneous system [3]. Thus, this extrapolation method does appear to be an effective technique for dealing with non-linear conditions during association rate constant measurements.

The last portion of this study examined the overall fit of the equations developed in this work to actual results obtained with a known heterogenous system. The model system used for this purpose was a mixed-bed affinity column that contained known amounts of protein A and protein G as ligands. Both of these proteins have strong binding to rabbit IgG under physiological conditions but have about a 1.5-fold difference in their association equilibrium constants for this solute [20,21]. In this work, it was found that these different binding affinities are partly due to these two ligands having different association rate constants for rabbit IgG, thus making them useful as models for studying ligand heterogeneity effects in split-peak measurements.

In the initial experimental studies, protein A and protein G were immobilized onto the same type of support and placed into separate columns of identical dimensions. Frontal analysis was then used to determine the value of m_{Ltot} for rabbit IgG on each support and controlled sample load experiments were used to generate split-peak plots for each type of column (e.g., see Figs. 1 and 2). Based on previous estimates of $1/\{k_1 V_e\}$ for rabbit IgG [2], it was possible to determine that both columns exhibited adsorption-limited behavior under the flow-rate conditions that were used in this study.

The slopes measured in the split-peak plots for the protein A and protein G columns were next plotted as a function of sample load, as discussed earlier for the simulation studies (see examples in Fig. 6). Using the known value of m_{Ltot} for each column and the extrapolated slopes obtained from graphs like those in Fig. 6, the apparent association rate constants for the protein A and protein G supports were

Table 1
Measured or predicted values for the association rate constants on protein A, protein G or mixed-bed protein A–protein G columns[a]

Type of column	Column binding capacity, $m_{L\text{tot}}$ (nmol)	Apparent association rate constant, k_3 ($M^{-1}\,s^{-1}$)
Protein A	0.26(±0.03)	$3.9(\pm 0.2)\cdot 10^6$
Protein G	0.71(±0.04)	$1.8(\pm 0.2)\cdot 10^6$
Protein A–protein G	0.37(±0.04)	$2.5(\pm 0.1)\cdot 10^6$ measured $2.9(\pm 0.3)\cdot 10^6$ predicted

[a] The values in parentheses represent a range of ±1 S.D..

determined (see results summarized in Table 1). It was found that recombinant protein G had a lower association rate constant than single binding domain recombinant protein A ($\beta_2 = k_{3,\text{Protein G}}/k_{3,\text{Protein A}} = 0.46$); however, both ligands had association rate constants that were larger than previously measured by the same approach for immobilized, intact recombinant protein A ($k_3 = 1.2\cdot 10^5\ M^{-1}\,s^{-1}$) [2]. These larger apparent rate constants are believed to be due to the decrease in or absence of steric hindrance between binding domains on the same ligand when using single binding domain protein A (with one IgG binding region) or protein G (with three binding sites) instead of intact protein A, which has up to four binding regions for rabbit IgG [20,21].

Both the protein A and protein G supports gave linear plots for $-1/\ln f$ versus flow-rate at each tested sample load (see examples in Fig. 2), with the slopes of these plots increasing with the amount of injected sample. For each of these ligands, good qualitative and quantitative agreement was seen in their observed split-peak behavior when compared to that predicted by the simulations. This was particularly true for the single binding domain protein A, which gave a sample load dependence essentially identical to that expected for a true homogeneous column (e.g., compare Fig. 5a and Fig. 6a). The protein G column's behavior also agreed well with that of the simulations, but this column gave slightly more curvature in its plot of measured slope versus sample load than would be expected for a true homogeneous ligand; this small difference in behavior is again thought to be due to the presence of more intra-ligand steric hindrance in the binding of IgG to protein G versus single binding domain protein A.

To further test the validity of the expressions and simulations used in this work to describe heterogeneous columns, split-peak plots were next generated for a column that contained a known mixture of the protein A and protein G supports. In this case, these supports were combined in a 3:1 ratio of protein A versus protein G to produce an equal amount of each ligand in the column ($\alpha_1 = \alpha_2 = 0.5$). The final binding capacity of the mixed-bed column was then confirmed by frontal analysis (see Table 1). A typical split-peak plot generated with this column in a controlled sample load experiment is shown in Fig. 2; such plots gave the same type of linear behavior as noted in the simulations for heterogeneous columns. A greater sample load dependence was observed for the mixed-column than for the protein A column, as predicted by the simulations (e.g., see Fig. 5). The observed change in slope for split-peak plots obtained with the mixed-bed column as the sample load was varied also gave behavior that agreed well with that seen in the simulations (e.g., compare Fig. 5b and Fig. 6b).

The final experiment in this study compared the apparent association rate constant that was measured for the mixed-bed column with that predicted by Eq. (14) based on the known rate constants and composition of the individual ligands in this column. For example, if the extrapolated slope of Fig. 6b is treated as a homogeneous system, then the apparent value of k_3 obtained from this slope will be related to the true rate constants of the system by the expression $k_{3,\text{app}} = k_{31}\{\alpha_1 + \beta_2 - \alpha_1\beta_2\}$, as indicated by a comparison of Eqs. (4) and (14). However, in this particular study the values of k_{31} (i.e., k_3 for protein A), α_1 and β_2 were already known (see previous paragraphs), thus providing an independent estimate for $k_{31}\{\alpha_1 + \beta_2 - \alpha_1\beta_2\}$. The predicted and measured values of $k_{3,\text{app}}$ obtained for the mixed-bed column are given in Table 1. Excellent agreement was seen between the theoretical and experimental apparent

rate constants, with these values overlapping within a range of ±2 S.D. and differing by less than 14% in value. This result further supports the validity of the models and equations used in this work to describe split-peak measurements in heterogeneous, adsorption-limited systems.

5. Conclusion

Although it has often been hypothesized that ligand heterogeneity plays an important role in split-peak measurements [2–4,8,9,14], this current study is the first time that this item has been examined in any detail at either the theoretical or experimental level. In this work, exact expressions were derived to describe the effects of ligand heterogeneity under linear elution conditions, and simulation models were developed to examine the combined effects of ligand heterogeneity and non-linear elution in systems with adsorption-limited rates for solute binding. The overall trends observed in the simulations indicated that ligand heterogeneity increases the amount of free solute seen at any flow-rate or sample size. This agrees with experimental observations made in this work and previous reports [2,3], thus supporting earlier speculations regarding the importance of column heterogeneity in split-peak studies.

One specific application in which the effects of ligand heterogeneity plus non-linear elution were examined concerned the use of the split-peak effect for association rate constant determinations. From the simulations, it was found that linear extrapolation methods developed for homogeneous systems (as a correction for non-linear elution conditions) could successfully be applied to columns containing heterogeneous ligands. The validity of this approach was further tested by using columns that contained immobilized protein A and/or protein G as experimental models. The behavior of these columns showed good quantitative and qualitative agreement with that predicted both for systems with homogeneous ligands (i.e., the individual protein A and protein G columns) or heterogeneous ligands (i.e., the mixed-bed protein A–protein G support). Overall, the results of this study provide a better understanding of the split-peak effect in real systems and allow for an improved quantitative description of this effect in its various applications.

6. List of symbols

[A]	molar concentration of solute
f	free or non-retained fraction of solute
F	volumetric flow-rate for sample injection
k_1	forward mass transfer rate constant for solute
k_{-1}	reverse mass transfer rate constant for solute
k_{3i}	second-order association rate constant for the binding of solute to ligand i
Load A	relative amount of solute injected versus the total column binding capacity, where Load A = moles solute/m_{Ltot}
$[\mathrm{L}_i]$	effective concentration of ligand i in the stagnant mobile phase, where $[\mathrm{L}_i] = m_{\mathrm{L}i}/V_{\mathrm{p}}$
$m_{\mathrm{L}i}$	moles of ligand i in the column
m_{Ltot}	total moles of ligand in the column, where $m_{\mathrm{Ltot}} = \Sigma m_{\mathrm{L}i}$
S_{o}	split-peak constant for a column, where $S_{\mathrm{o}} = F/(k_{31} m_{\mathrm{Ltot}})$ for a homogeneous system with adsorption-limited kinetics or $S_{\mathrm{o}} = F/(k_{31} m_{\mathrm{Ltot}} \Sigma\{\alpha_{\mathrm{i}} \beta_{\mathrm{i}}\})$ for a system with heterogeneous ligands and adsorption-limited kinetics
V_{e}	excluded volume of column; volume of flowing mobile phase
V_{p}	pore volume of column; volume of stagnant mobile phase
α_i	relative fraction of ligand i versus all other ligands in the column, where $\alpha_i = m_{\mathrm{L}i}/m_{\mathrm{Ltot}}$
β_i	ratio of solute association rate constant for ligand i versus the ligand with the highest association rate constant (L_1), where $\beta_i = k_{3i}/k_{31}$

Acknowledgements

This work was supported by the National Institutes of Health under grant no. R29 GM44931.

Appendix A

The methods and procedures used in the deriving Eqs. (9)–(11) were similar to those outlined in Ref. [2] for the homogeneous case. In this approach, the term x represents the distance travelled by solute from the top of the column bed ($x=0$) to any point along the total length of the column (h). The functions $p(x,t)$, $q(x,t)$ and $r(x,t)$ are used to describe the probabilities of finding solute at position x and time t in the flowing mobile phase, stagnant mobile phase or stationary phase regions; the following reactions represent the transfer of solute between these three regions.

$$p \underset{k_{-1}}{\overset{k_1}{\rightleftarrows}} q \tag{A1}$$

$$q \xrightarrow{\Sigma\{k_{3i}[L_i]\}} r \tag{A2}$$

By using conservation of mass, the partial differential equations shown in Eqs. (A3)–(A5) can be obtained for describing the transfer of solute between these various probability states

$$\partial p/\partial t = u_e(\partial p/\partial x) - k_1 p + k_{-1} q \tag{A3}$$

$$\partial q/\partial t = k_1 p - k_{-1} q - \left(\sum \{k_{3i}[L_i]\}\right) q \tag{A4}$$

$$\partial r/\partial t = \left(\sum \{k_{3i}[L_i]\}\right) q \tag{A5}$$

where u_e is the linear velocity of an excluded, non-retained solute (i.e., the flowing mobile phase velocity) and all other terms are as defined earlier. If the initial layer of solute at the top of the column is considered sufficiently small to be described by a Dirac delta function, or a series of delta function inputs, then the initial column conditions for $0 \le x \le h$ are given by the statements $p(x,0)=\delta(x-h)$, $q(x,0)=0$ and $r(x,0)=0$. Furthermore, since there are no solute molecules at the top of the column bed when the initial layer leaves, the boundary conditions for $t>0$ are given by $p(h,t)=0$, $q(h,t)=0$ and $r(h,t)=0$.Based on the given boundary conditions, one can integrate Eqs. (A3)–(A5) with respect to time to obtain the following relationships:

$$u_e \partial/\partial x \int_0^\infty p(x,t)\,dt = -\delta(x-h) - k_1/\left(1 + k_{-1}/\sum\{k_{3i}[L_i]\}\right)\int_0^\infty p(x,t)\,dt \tag{A6}$$

$$r(x,\infty) = \sum\{k_{3i}[L_i]\}\int_0^\infty q(x,t)\,dt = k_1\int_0^\infty p(x,t)\,dt - k_{-1}\int_0^\infty q(x,t)\,dt \tag{A7}$$

$$\int_0^\infty q(x,t)\,dt = k_1/(k_{-1} + \Sigma\{k_{3i}[L_i]\})\int_0^\infty p(x,t)\,dt \tag{A8}$$

If one lets $y=h-x$ and uses Laplace transforms to solve the above equations based on the given boundary conditions, the results in Eqs. (A9) and (A10) are obtained

$$\int_0^\infty u_e\,p(x,t)\,dt = e^{-c(h-x)} \tag{A9}$$

$$r(x,\infty) = c\,e^{-c(h-x)} \tag{A10}$$

where c represents the following combination of constants.

$$c = (k_1/u_e)/\left(1 + k_{-1}/\sum\{k_{3i}[L_i]\}\right) \tag{A11}$$

By using the above expressions, the relationships shown in Eqs. (A12) and (A13) are obtained and can be used to determine the free fraction f for the solute:

$$f = \int_0^\infty u_e\,p(0,t)\,dt = e^{-ch} \tag{A12}$$

or

$$-1/\ln f = u_e/h\left[1/k_1 + k_{-1}/\left(k_1\sum\{k_{3i}[L_i]\}\right)\right] \tag{A13}$$

The final expressions shown in Eqs. (9) and (10) are then obtained from Eq. (A13) by substituting in F/V_e for u_e/h and using the fact that $k_1/k_{-1}=V_p/V_e$. Eq. (11) for the adsorption-limited case is derived in a similar fashion by making the same substitutions and

dropping the mass transfer term from the right-hand side of Eq. (A13).

References

[1] A.M. Katti, G.A. Guiochon, Adv. Chromatogr. 31 (1991) 1.
[2] D.S. Hage, R.R. Walters, H.W. Hethcote, Anal. Chem. 58 (1986) 274.
[3] D.S. Hage, R.R. Walters, J. Chromatogr. 436 (1988) 111.
[4] J.L. Wade, P.W. Carr, J. Chromatogr. 449 (1988) 53.
[5] A. Jaulmes, C. Vidal-Madjar, Anal. Chem. 63 (1991) 1165.
[6] H. Place, B. Sebille, C. Vidal-Madjar, Anal. Chem. 63 (1991) 1222.
[7] J.C. Giddings, H. Eyring, J. Phys. Chem. 59 (1955) 416.
[8] R. Sportsman, J.D. Liddil, G.S. Wilson, Anal. Chem. 55 (1983) 771.
[9] D.S. Hage, R.R. Walters, J. Chromatogr. 386 (1987) 37.
[10] L.A. Larew, R.R. Walters, Anal. Biochem. 164 (1987) 537.
[11] C. Vidal-Madjar, H. Place, L. Boulkanz, A. Jaulmes, J. Chromatogr. 548 (1991) 81.
[12] D.S. Hage, D.H. Thomas, M.S. Beck, Anal. Chem. 65 (1993) 1622.
[13] J.P. McConnell, D.J. Anderson, J. Chromatogr. 615 (1993) 67.
[14] J. Renard, C. Vidal-Madjar, J. Chromatogr. A 661 (1994) 35.
[15] D.H. Thomas, M. Beck-Westermeyer, D.S. Hage, Anal. Chem. 66 (1994) 3823.
[16] P.F. Ruhn, J.D. Taylor, D.S. Hage, Anal. Chem. 66 (1994) 4265.
[17] J.G. Rollag, M. Beck-Westermeyer, D.S. Hage, Anal. Chem. 68 (1996) 3631.
[18] H.W. Hethcote, C. DeLisi, J. Chromatogr. 248 (1982) 183.
[19] J.I. Steinfield, J.S. Francisco, W.L. Hase, Chemical Kinetics and Dynamics, Prentice–Hall, Englewood Cliffs, NJ, 1989.
[20] B. Akerstrom, L. Bjorck, J. Biol. Chem. 261 (1986) 10240.
[21] S. Jonsson, G. Kronvall, Eur. J. Immunol. 4 (1974) 29.